

Comparison of surface and canopy urban heat islands within megacities of eastern China

Yonghong Hu^{a,b,1}, Meiting Hou^{c,1}, Gensuo Jia^{d,*}, Chunlei Zhao^b, Xiaoju Zhen^b, Yanhua Xu^e

^a Key Laboratory of Digital Earth Science, Aerospace Information Research Institute, Chinese Academy of Sciences, Beijing 100094, China

^b Key Laboratory of Meteorology and Ecological Environment of Hebei Province, Shijiazhuang 050021, China

^c China Meteorological Administration Training Centre, China Meteorological Administration, Beijing 100081, China

^d Key Laboratory of Regional Climate-Environment for East Asia, Institute of Atmospheric Physics, Chinese Academy of Sciences, Beijing 100029, China

^e Xinlian College of Henan Normal University, Zhengzhou 450000, China



ARTICLE INFO

Keywords:

Urban heat island
Land use
Climate background
Urbanization

ABSTRACT

Urban heat island (UHI) can be characterized and quantified to understand the modification of urban surfaces on the local and regional climate. This study examines UHI variation across three megacities that are located in rapid urbanization regions in eastern China (Beijing, Shanghai and Guangzhou). These cities are located within a warm temperate climate zone, north subtropical climate zone, and lower subtropical climate zone, respectively. Satellite-based land surface temperature (LST) data and air temperature records from 2003 to 2016 were used to identify surface urban heat island (SUHI) and canopy urban heat island (CUHI), respectively. Generally, the average annual SUHI is higher than the CUHI, with the greatest UHIs appearing in Beijing (SUHI: $2.33 \pm 0.18^\circ\text{C}$, CUHI: $1.45 \pm 0.54^\circ\text{C}$). UHI changes across latitudes were negatively related to humidity variation, with higher UHI in drier climates. Seasonal UHI analysis suggests that a lower SUHI would occur in winter and a higher UHI in spring and summer, except for Guangzhou. CUHI in dry season was higher than in wet season for all three megacities, and the largest CUHI ($2.10 \pm 0.33^\circ\text{C}$) appeared in winter in Beijing. Various patterns of seasonal cycles of SUHI and CUHI were related to monthly precipitation and solar insolation. Annual average daytime SUHI was higher than the nighttime SUHI, and larger daytime SUHI appeared in Guangzhou, contrasting with Shanghai and Beijing. The difference between SUHI and CUHI for all seasons was also high in Guangzhou. UHI changes were considered to be altered by warm and wet conditions in mega-cities of eastern China, and heat transportation from urban surface to urban canopy provided some possible understanding of the UHI change.

1. Introduction

More than 55% of the world's population lived in cities in 2018, and the trend of people moving into town will continue as rapid urbanization in many developing countries (United Nations, 2018). Urbanization has caused the conversion of natural surface to impervious surface, which permanently changed land surface properties in mass and energy exchange between urban and atmosphere (Voogt and Oke, 2003). Changes in land use and cover formation, along with the urban canopy structure usually lead to an increase in urban heat storage and heat within the atmosphere (Arnfield, 2003; Hu et al., 2016), which shape the local climate and result in urban heat island effect (UHI), the well-known difference of surface temperature between urban and rural area (Arnfield, 2003; Jin, 2012; Voogt and Oke, 2003). According to their

characterization in different layers of urban atmosphere, urban heat island is divided into three categories: surface urban heat island (SUHI), canopy urban heat island (CUHI) and boundary urban heat island (BUHI) (Voogt and Oke, 2003; Yuan and Bauer, 2007). The BUHI is relatively hard to detect due to temperature difference from sensors mounted on tall towers, balloons and aircraft (Voogt and Oke, 2003), and climate model simulation has been usually used to understand the characterization of BUHI (Baik et al., 2007; Miao et al., 2009). Most studies have focused on the characterization of urban heat island in urban surface and urban canopy layers (Arnfield, 2003).

Canopy urban heat island is usually quantified by air temperature records from urban and rural stations (Camilloni and Barros, 1997; Stewart and Oke, 2012). Studies from meteorological measurements and model simulations both indicate that UHI has seasonal and diurnal

* Corresponding author.

E-mail addresses: huyh01@radi.ac.cn (Y. Hu), jiong@tea.ac.cn (G. Jia).

¹ These authors contributed equally to this work.

variations (Arnfield, 2003; Gedzelman et al., 2003). However, limits of UHI measured by station records were also claimed by researches about how to select the typical urban and rural station (Jin, 2012; Mohsin and Gough, 2012). The heterogeneous time series of air temperature records usually result in uncertainties of warming trend induced by urbanization process (Stewart and Oke, 2012; Wu and Yang, 2013; Yan et al., 2010). The universal classification system of “local climate zone” (LCZ) was proposed to address the inadequacies of urban–rural description for the inter-comparison of UHI results from different researches (Stewart and Oke, 2012).

Satellite-based land surface temperature (LST) is widely used in the monitoring of SUHI (Lazzarini et al., 2013; Streutker, 2003; Huang and Wang, 2019) and can provide detailed information in regards to surface temperature variation over various land cover types (Chen et al., 2006; Lazzarini et al., 2013; Weng et al., 2004). Land surface temperature derived from satellite images was considered as an effective way to improve the spatial variation of CUHI process due to its advantages in spatial observation (Hu and Jia, 2010; Jin, 2012; Voogt and Oke, 2003; Weng et al., 2004). However, satellite-based LST products should be used with caution because quality control flags of satellite products have obvious impacts on UHI (Lai et al., 2018).

Green vegetation can alter UHI intensity by decreasing surface temperature, while dense settlement regions or central business districts usually have higher surface temperatures (Hu and Jia, 2010; Lazzarini et al., 2013). Several indices were developed to examine the impact of urbanization process on UHI in detail, such as the Normalized Difference Vegetation Index (NDVI), Normalized Difference Built up Index (NDBI) and impervious surface fraction (ISF) (Chen et al., 2006; Hu and Jia, 2010; Yuan and Bauer, 2007). In order to minimize the potential environmental impacts of urbanization, fractional composition and structural properties of the urban landscape were also used to understand how landscape structure affects the local climate by exploring the relationship between surface temperature and land use patterns (Buyantuyev and Wu, 2010; Li et al., 2011). UHI has already become a major concern as it not only intensifies extreme weather events (Holderness et al., 2013; Hu and Jia, 2010), but also enhances air pollution (Holderness et al., 2013; Hu and Jia, 2010; Sarrat et al., 2006; Zhao et al., 2014).

UHI changes can be altered by many local environmental factors, such as urban morphology (Huang and Wang, 2019), urban green space, impervious surface land fraction or land use/cover change. The increase of urban green space could cause lower surface temperature due to its higher evapotranspiration and less emissivity than urban impervious surface (Elmes et al., 2017; Maimaitiyiming et al., 2014), which effectively mitigated urban heat island effect (Chen et al., 2006; Weng et al., 2015). Vegetation index and impervious surface were also considered as the indicators for surface urban heat island (Yuan and Bauer, 2007). Indeed, urbanization usually resulted in more urban impervious surface and complex urban morphology, which could change land surface properties and capture more solar radiation, and then intensify urban heat island (Voogt and Oke, 1998; Hu and Jia, 2010; Tran et al., 2017; Weng, 2012). Global investigation for urban SUHI intensities also showed different patterns of SUHI intensity along different latitudes with different climate background information (Peng et al., 2012). Fu and Weng (2018) further noted that SUHIs and differences in annual temperature cycle between urban and rural areas could be influenced by different climate zones. Zhao et al. (2014) used climate model to find that humidity situation in different climate background was an important factor altering surface temperature variation. The interactions between UHIs and regional/global climate change further highlighted that identification of UHI patterns in different climate background would help understand their contribution to global climate change and the synchronicity characterization between UHI growth and climate change (Bornstein et al., 2012).

Urban heat island is a complex phenomenon that can be altered by both natural and social environment. The comparison of UHI across

different regions is important to understand the corresponding change influenced by micro and macro-scale social and natural factors. The investigation of SUHI and CUHI will also provide some suggestions on ways to mitigate the impact of extreme urban climate on human health. However, limitations still exist in previous studies on UHI comparisons in different regions. It is challenging to identify UHI evolution from urban surface to urban canopy over different latitudes, with uncertainties from heterogeneous meteorological records, limitations of urban and rural site identification, and inconsistent coverage of satellite-based datasets (Stewart and Oke, 2012; Stewart, 2011; Hu and Brunsell, 2013; Wang et al., 2017). Therefore, this study tried to examine surface and canopy UHI variation from 2003 to 2016 in three typical mega-cities of eastern China by using temporal aggregated satellite-based surface temperature and air temperature records, and further compare the average SUHI and CUHI in different megacities in order to understand patterns of UHI under relative social and natural environments.

2. Methods

2.1. Selection of mega-cities in eastern China

Large cities in eastern China have experienced rapid urbanization with the conversion of large area of natural land to impervious surface since the Reform and Open-door Policy starting in the early 1980s. Three typical mega-cities in eastern China (Beijing, Shanghai and Guangzhou) were selected to examine UHI variation (Fig. 1). The three cities have differing climatic properties with annual mean temperature of 14 °C, 16 °C and 22 °C respectively and annual precipitation of 500 mm, 1200 mm and 1600 mm respectively. Meanwhile, they have already become regional economic centers with large amount of people. According to urban population change over the last decades, these cities have experienced rapid urbanization with the urbanization rate greater than 85% in 2016. These cities have clear urban cores with intensive urban buildings and some small satellite towns in the surrounding areas (Fig. 1).

2.2. Urban land use detection

National land use/cover dataset of China (NLCD) from the 1980s to 2015 has been developed by the Chinese Academy of Sciences, and it has become a main source of authoritative data for land use and cover change studies in the late 2000s within China (Liu et al., 2005; Zhang et al., 2014). This study selected the dataset at 1:100000 scale (Zhang et al., 2014) to examine urban land use in three mega-cities. These land use products were derived from Landsat images and provided fractional percentages of each land cover type within 1 km grids. A hierarchical classification system was conducted for NLCD product with six first-level classes and 25 second-level classes, and overall accuracy of first-level classes greater than 95% in 2010 (Liu et al., 2005; Zhang et al., 2014). This study selected 6 first-level classes to examine land use properties, including cropland, woodland, grassland, water bodies, urban and built-up areas, and unused land. Here, urban and built-up was used to delineate regions that were used for settlements, factories and transportation facilities, which represent the horizontal urban surface with the development intensity as a function of the extent and spatial distribution of the collection of man-made surfaces within a pixel.

2.3. Identification of urban and rural stations

In order to identify urban and rural stations, we first distinguished between urban and rural land along an urban–rural gradient using a City Clustering Algorithm (Peng et al., 2012). For each pure urban pixel from land use datasets, we identified urban land according to the criterion that the land cover type of 8-neighbors of the given pixel is urban

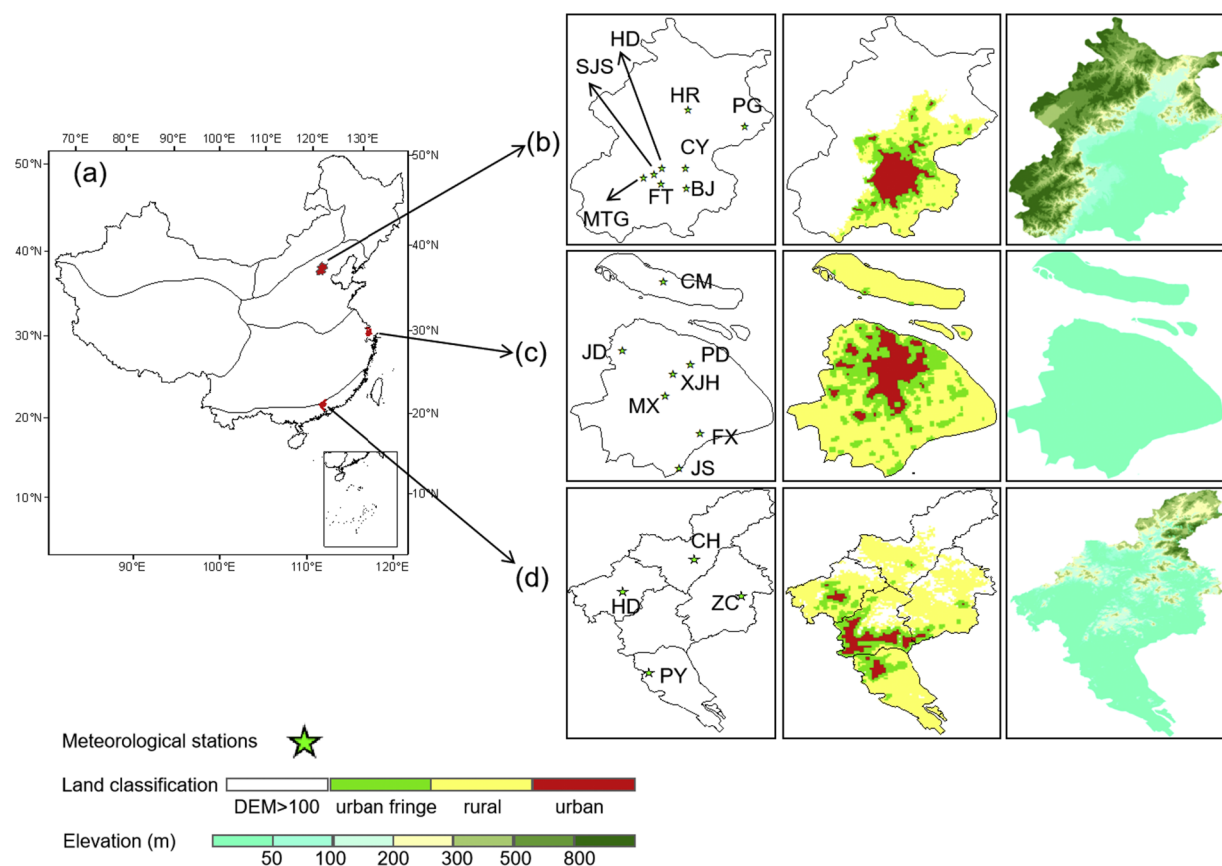


Fig. 1. Location of study area (a), Beijing (b), Shanghai (c) and Guangzhou (d), and the distribution of urban and rural stations in three mega-cities (see the details of stations in Table 1). Three cities are located at warm temperate climate zone, north subtropical climate zone and lower subtropical climate zone, respectively. Urban and rural stations with elevation less than 100 m were identified to derive and compare CUHIs in three mega-cities.

land, and then aggregated those pixels as urban. Then, the 3×3 moving window was conducted for other regions to identify urban fringe with more than 4 pixels of each window belonging to urban land. Other regions surrounding urban areas, including large area of crop-land, woodland, grassland and water, were considered as rural surface.

To ensure the representative of urban and rural stations, we further investigated the stations and their surrounding areas by using DEM, land use datasets and Google Map information, under the condition that the 8-neighbors of the selected station pixel were pure type of urban or rural land cover. Specifically, we first removed the stations with altitude greater than 100 m to reduce topographical influence in UHI derivation. Those stations distributed at urban fringe were also removed due to their mixed land surface characteristics. Then, the sites where relocation occurred from 2003 to 2016 were removed in this study, such as Guangzhou station in 2011. Finally, relative stable urban and rural stations were selected to derive CUHI, including 19 stations in three mega-cities (Table 1).

2.4. UHI derived from satellite datasets and site observation records

2.4.1. Surface UHI from satellite-based LST

In order to examine the annual UHI difference, we selected 8-day composite land surface temperature (LST) products (MOD11A2 and MYD11A2) from the MODIS sensor boarded at the Terra and Aqua satellite platform. MODIS is sun-synchronous and provides four observations per day for nearly every place on Earth, including daytime (about local solar time 10:30 AM from Terra and 13:30 PM from Aqua) and nighttime (about 22:30 PM from Terra and 01:30 AM from Aqua) observations. LST products have been proved to be of high quality in identifying surface thermal characterization with an accuracy of less

Table 1

The selected stations in Beijing, Shanghai and Guangzhou for CUHI detection from 2003 to 2016

City	Number	Station	Station type
Beijing	1	Huairou (HR)	Rural
	2	Pinggu (PG)	Rural
	3	Chaoyang (CY)	Urban
	4	Haidian (HD)	Urban
	5	Beijing (BJ)	Urban
	6	Fengtai (FT)	Urban
	7	Shijingshan (SJS)	Urban
	8	Mentougou (MTG)	Rural
Shanghai	1	Congming (CM)	Rural
	2	Jiading (JD)	Rural
	3	Pudong (PD)	Urban
	4	Xujiahui (XJH)	Urban
	5	Minxing (MX)	Urban
	6	Fengxian (FX)	Rural
	7	Jinshan (JS)	Urban
Guangzhou	1	Conghua (CH)	Rural
	2	Huadu (HD)	Urban
	3	Zengcheng (ZC)	Rural
	4	Panyu (PY)	Rural

than 1 K by using improved day and night algorithms and removing of could contamination (Wan, 2008). The tiles of original MODIS data were geo-corrected, re-projected and combined to generate spatial mosaic LST datasets within the study area. Satellite images from four scanning times of Terra and Aqua were processed to examine the diurnal variation of LST change and generate annual and seasonal LST from 2003 to 2016. The traditional meteorological definition of seasons

was used in considering MAM (March, April and May) as spring, JJA (June, July and August) as summer, SON (September, October and November) as autumn and DJF (December, January and February) as winter. In contrast to air temperature from site observation, satellite-based LST has an advantage of large areal coverage.

2.4.2. Canopy UHI from air temperature records

We used the 19 weather stations of three mega-cities (Table 1) to collect air temperature records with observation time period from 2003 to 2016. The location of these stations was also shown in Fig. 1. These stations were established by China Meteorological Administrations (CMA), including the basic reference station, basic station and reference station. Strict quality control has been conducted by CMA for the consistence of air temperature records.

3. Results and discussion

3.1. SUHI variation of three mega-cities

Satellite-based LST from 2003 to 2016 were used to examine the magnitude of surface temperature variation within the entire metropolitan area and spatial extent of surface heat island (Fig. 2). LSTs in Beijing ranged from 6.68 to 21.19 °C, 16.13 to 31.00 °C, 5.16 to 17.55 °C, and –10.02 to 2.06 °C, with average values of 14.87 °C, 24.47 °C, 11.86 °C and –2.73 °C in spring, summer, autumn, and winter respectively (Table 2). As expected, Shanghai displayed similar seasonal LSTs ranging from 13.74 to 23.04 °C, 23.53 to 31.21 °C, 16.82 to 24.58 °C, and –2.38 to 8.91 °C, with average values of 17.44 °C, 27.84 °C, 19.12 °C and 6.58 °C in spring, summer, autumn, and winter respectively. The LSTs of Guangzhou were higher than Beijing and Shanghai, ranging from 18.05 to 26.77 °C, 22.28 to 30.76 °C, 18.53 to 26.85 °C, and 11.35 to 18.94 °C, with average values of 22.49 °C, 26.89 °C, 22.95 °C and 15.47 °C in spring, summer, autumn, and winter respectively.

Spatial variation of LST over different zones of three mega-cities revealed variation in the UHI. High LST regions are mainly concentrated in urban built-up areas and their satellite towns. The hot-spots for UHI were predominantly found in urban cores where built-up areas included densely populated districts, such as the Haidian district

Table 2

Seasonal variation of land surface temperature (°C) in Beijing, Shanghai and Guangzhou

	Beijing	Shanghai	Guangzhou
Spring	14.87	17.44	22.49
Summer	24.47	27.84	26.89
Autumn	11.86	19.12	22.95
Winter	–2.73	6.58	15.47

in Beijing, Liwan district in Guangzhou, and Jingan district in Shanghai.

When comparing the difference of annual mean SUHI intensity among Beijing, Shanghai and Guangzhou, the trend of SUHI changes along the climate-based gradient was found. Mega-cities with warm, wet climates in southern China tend to have a lower UHI than cities with cool, dry climates in northern China. For example, SUHI reached 2.21 ± 0.26 °C in Guangzhou, compared with 2.30 ± 0.15 °C in Beijing. Annual mean SUHI intensity in Shanghai (2.18 ± 0.13 °C) was lower than Beijing and higher than Guangzhou. LST change was highly correlated with urban land fraction, with high LSTs appearing within more intensive urban building regions, while low temperature regions were concentrated in the dense vegetation areas. High temperature spots usually occurred within city limits and their satellite towns with large populations, dense building and strong anthropogenic heat release (Yu et al., 2005; Feng et al., 2010).

SUHI intensity tended to be strong in summer and weak in winter in all three cities (Table 3). An increasing trend from south to north was detected for aggregated summer SUHI with the largest summer SUHI in Beijing reaching 3.39 ± 0.28 °C. Other studies have also found that UHI is typically higher in summer and lower in winter, and summer UHI has resulted in severe impacts on human health, urban energy consumption and local climate change, along with heat waves and extreme events of high temperature (Holderness et al., 2013). However, the summer SUHI is lower in Guangzhou, which could be related to higher precipitation (about 834 mm). An increase in precipitation tends to result in greater soil moisture. Soil moisture of rural surfaces in wet or dry climates can influence UHI intensity, as it is slower for wet soil to heat up or cool down, compared to dry surfaces in rural areas (Bornstein et al., 2012). Therefore, lower summer SUHI in Guangzhou

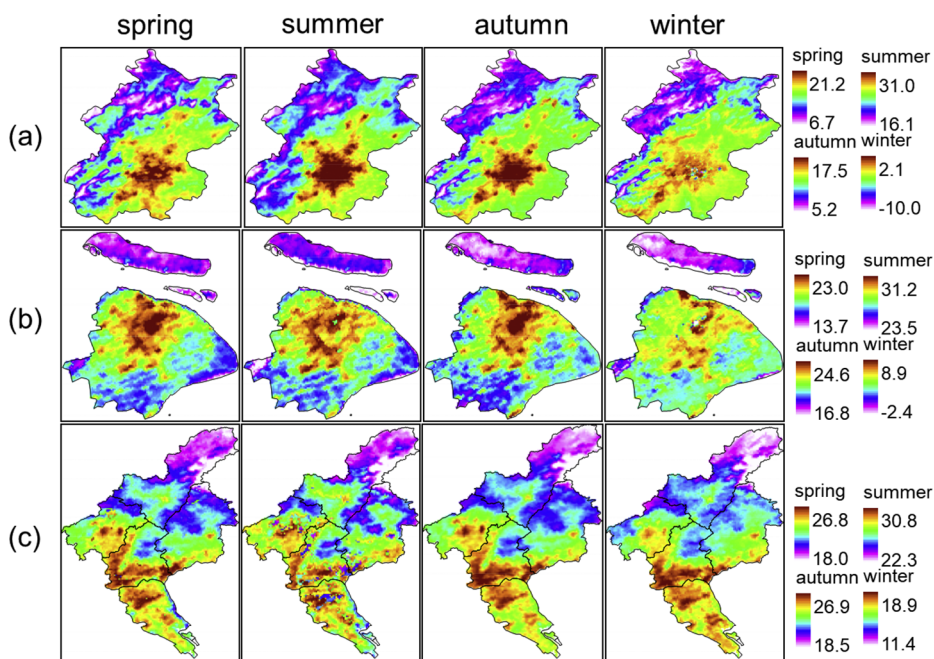


Fig. 2. Spatial patterns of seasonal SUHI (°C) variation in Beijing (a), Shanghai (b) and Guangzhou (c).

Table 3

Seasonal average SUHI ($^{\circ}\text{C}$) over Beijing, Shanghai and Guangzhou from 2003 to 2016.

	Spring	Summer	Autumn	Winter
Beijing	2.00 ± 0.29	3.39 ± 0.28	2.24 ± 0.13	1.55 ± 0.16
Shanghai	2.90 ± 0.20	2.57 ± 0.41	2.21 ± 0.16	1.06 ± 0.16
Guangzhou	2.35 ± 0.48	2.16 ± 0.71	2.48 ± 0.23	1.85 ± 0.21

than in Beijing and Shanghai was partly caused by wetter soil moisture conditions related to higher precipitation.

The opposite trend was observed for the average daytime SUHI and nighttime SUHI variation within the three megacities along the latitude gradient (Table 4). Average daytime SUHI at the southern areas was higher than cities at the northern areas. For example, daytime SUHI at Guangzhou reached to $2.60 \pm 0.52^{\circ}\text{C}$, while Beijing was $1.58 \pm 1.97^{\circ}\text{C}$. In contrast, mean nighttime SUHI in Guangzhou was lower than that of Beijing by 1.19°C . These trends were not evident between Shanghai and Guangzhou. Mean daytime SUHI in Beijing was lower than the mean nighttime SUHI by 1.43°C , while daytime SUHI was higher than nighttime SUHI in Shanghai and Guangzhou by 1.54°C and 0.78°C respectively. Seasonal variation of aggregated monthly daytime and nighttime SUHI from 2003 to 2016 was also examined (Fig. 3). The peak daytime SUHI occurred in various months, with Beijing in August, Shanghai in May and Guangzhou in October. The SUHI peak in Beijing ($5.16 \pm 0.66^{\circ}\text{C}$) was higher than that of Guangzhou and Shanghai. In comparison, a lower magnitude of SUHI fluctuation was observed at night. Daytime SUHI was higher than nighttime SUHI from June to September in Beijing. This phenomenon could be extended to the period of February to October in Shanghai, or the whole year in Guangzhou. The difference in day and night SUHI intensity across southern and northern cities of China is consistent with other studies, as high night SUHI intensity in southern cities contrasts with low night SUHI in northern cities (Wang et al., 2015).

3.2. Comparison of CUHI and SUHI in three mega-cities

3.2.1. The difference between annual mean CUHI and SUHI

We analyzed the difference between annual mean CUHI and SUHI across three mega-cities from 2003 to 2016. SUHI and CUHI reached $2.21 \pm 0.26^{\circ}\text{C}$ and $0.89 \pm 0.58^{\circ}\text{C}$ in Guangzhou respectively, in contrast to $2.30 \pm 0.15^{\circ}\text{C}$ and $1.45 \pm 0.54^{\circ}\text{C}$ in Beijing. Annual mean SUHI and CUHI intensity in Shanghai ($2.18 \pm 0.13^{\circ}\text{C}$ and $0.93 \pm 0.41^{\circ}\text{C}$) was higher than Beijing and lower than Guangzhou. Some studies found that hot climates in low-latitude regions may result in a lower UHI, particularly during the wet seasons (Roth 2007). This can be due to relatively large thermal energy absorption of wet soil in rural surface, which reduces rural cooling and results in a smaller daily surface temperature range in rural areas. In addition, special urban morphology in these regions may cause less radiation absorption in urban regions (Roth, 2007; Oke et al., 1991).

Annual mean SUHI intensity was higher than annual mean CUHI across the three mega-cities. The difference between SUHI and CUHI in Beijing (1.63°C) was lower than Shanghai (1.74°C) and Guangzhou (1.69°C). This could be due to LST in urban regions having higher air temperatures than rural regions. For example, the mean annual urban

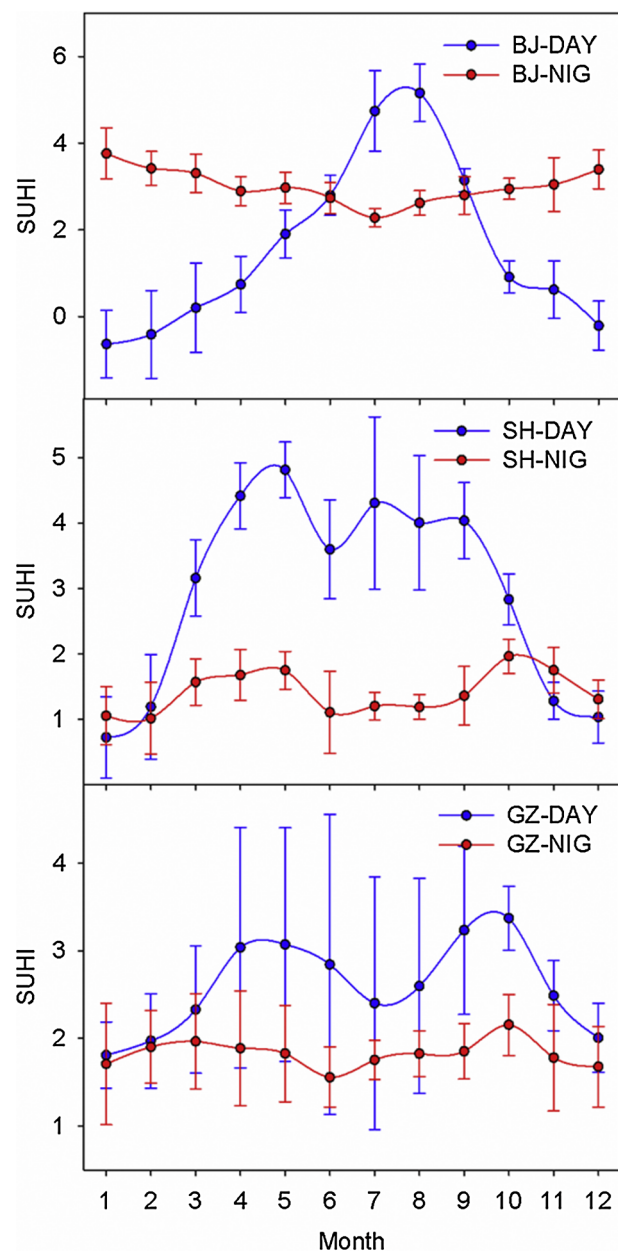


Fig. 3. Monthly mean daytime (DAY) and night (NIG) SUHI ($^{\circ}\text{C}$) in Beijing (a), Shanghai (b) and Guangzhou (c) from 2003 to 2016.

LST in Beijing reached 15.49°C , compared to 13.28°C in the rural regions. The horizontal energy transportation by atmospheric advection may also decrease the extent of air temperature change (Voogt and Oke, 2003). LST is usually higher than air temperature during the daytime and lower than air temperature during the night due to its variation highly related to the absorption of solar radiation on the surface (Jin and Dickinson, 2010), which indicates that LST has a larger amplitude of diurnal temperature cycle than air temperature.

Table 4

Averaged daytime and nighttime SUHI ($^{\circ}\text{C}$) over Beijing, Shanghai and Guangzhou from 2003 to 2016.

	Day			Night		
	Beijing	Shanghai	Guangzhou	Beijing	Shanghai	Guangzhou
Mean SUHI	1.58	2.95	2.60	3.01	1.41	1.82
Std.	1.97	1.50	0.52	0.40	0.32	0.15

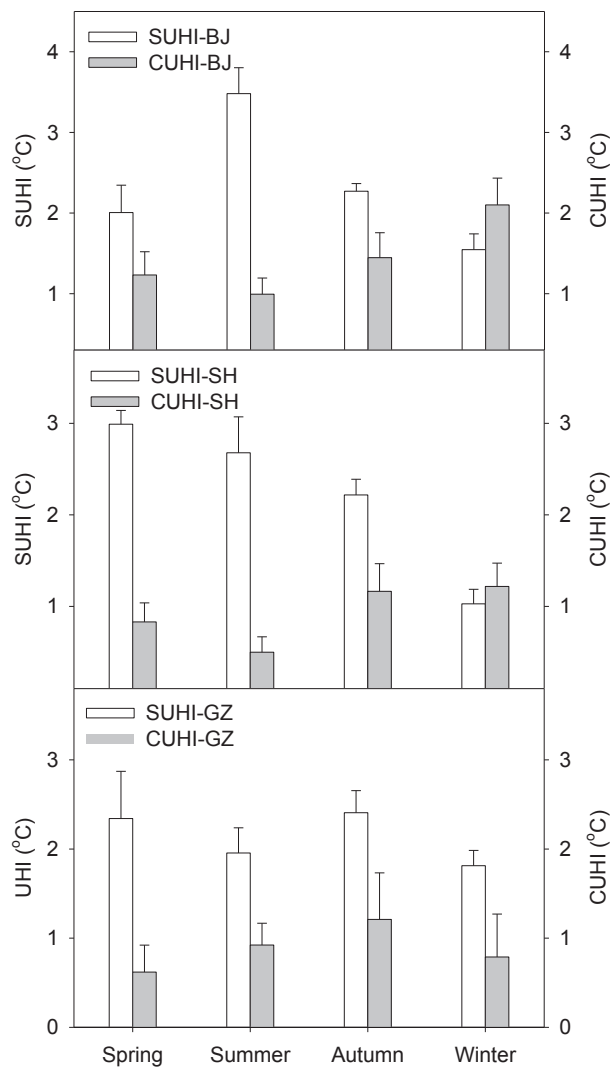


Fig. 4. The comparison of seasonal SUHI (°C) and CUHI in Beijing (BJ), Shanghai (SH) and Guangzhou (GZ) from 2003 to 2016.

3.2.2. Seasonal characterization of SUHI and CUHI in the three mega-cities

A seasonal profile of SUHI and CUHI across three mega-cities (Fig. 4) indicated that there were different patterns for CUHI and SUHI change across latitudes. SUHI was higher than CUHI during the spring, summer and autumn, while CUHI was higher than SUHI for winter in Beijing. The largest variation between SUHI and CUHI occurred in summer (2.48 °C), while SUHI in winter was lower than CUHI by 0.55 °C. The seasonal cycle of UHI displayed a trend of high SUHI within the summer, moderate SUHI in autumn and spring, and low in winter, contrasting with a higher CUHI in autumn and winter. A clear reverse pattern was detected in summer and winter between SUHI and CUHI. The highest SUHI was in summer (3.48 ± 0.32 °C) and lowest SUHI in winter (1.54 ± 0.19 °C), whereas the highest CUHI was in winter (2.10 ± 0.33 °C) and the lowest CUHI in summer (0.99 ± 0.20 °C). The controlling factors for UHI are usually attributed to the variation in land surface properties and anthropogenic heat

release in urban and rural areas (Stewart and Oke, 2012). Higher winter CUHI in Beijing may have been influenced by large heat release through the use of electrical power for heating and the burning of fossil fuels (Liu et al., 2007; Yu et al., 2005). Meanwhile, reduced solar heating in winter may further reduce the vertical turbulent transport and the boundary layer depth (Liu et al., 2007). Theoretically, CUHI in summer is low, probably because of the rainy season and more than 75% rainfall appeared in June and August, and wet days also reduce the amplitude of UHI (Roth, 2007).

The seasonal cycle of UHI variation in Shanghai was similar with that in Beijing. SUHI was higher than CUHI during the spring, summer and autumn. The largest variation between SUHI and CUHI occurred in summer (2.18 °C), while SUHI in winter was slightly lower than CUHI by 0.19 °C. The intensity of SUHI in Shanghai gradually decreased from spring to winter, and the highest CUHI was apparent in autumn (1.21 ± 0.25 °C). Shanghai has a subtropical climate, with wet season occurring from May to October. It is located near the East China Sea, making its climate highly influenced by the ocean winds. Higher SUHI in spring and summer than autumn and winter was concordant with other studies. These suggested that the main influence was anthropogenic heat release and landscape structure differences in urban and rural areas (Li et al., 2011; Jin et al., 2011). CUHI in Shanghai could be highly influenced by seasonal climate, such as strong winds and increased cloud cover reducing UHI effects in summer, and reduced wind and increased clear days intensifying UHI in autumn (Chen et al., 2003).

The difference between SUHI and CUHI in Guangzhou was obvious in all seasons, and the largest variation between them occurred in spring (1.98 °C). Autumn is the traditional dry season in southern China under subtropical climate, and the largest CUHI and SUHI in Guangzhou happened in autumn by 1.21 ± 0.52 °C and 2.41 ± 0.25 °C respectively. SUHI variation in Guangzhou was highly influenced by surface land properties with higher LSTs from dense buildings, while urban expansion also resulted in a SUHI increase from urban to suburban (Hu and Jia, 2010; Weng, 2003). However, these factors are not usually controllable in summer (wet season) due to strong winds, heavy rain and large cloud cover, leading to the rapid decrease or transportation of accumulative energy in urban regions (Wu et al., 2011). Therefore, the cumulative difference between urban and rural areas in summer is lower than other seasons. CUHI intensity in dry seasons (e.g. autumn) is usually higher than wet seasons (e.g. summer) in subtropical cities (Roth, 2007).

3.3. Influence of climate background of megacities on UHI across latitudes

UHI is considered to be influenced by many local factors, including urban expansion, surface heat storage induced by building materials, urban morphology with complex canyon geometry, solar radiation budget with a decrease of net longwave loss, anthropogenic heat release and urban green cover (Yuan and Bauer, 2007; Jin et al., 2011; Li et al., 2011; Voogt and Oke, 2003). UHI evolution depends on surface temperature difference between urban and rural areas. Surface temperature variation is highly correlated to land properties with a relatively stable physical characterization in urban land, with numerous impervious surfaces, whereas rural land properties are greatly influenced by soil moisture. Therefore, precipitation and relative humidity can be used to examine whether UHI variation is influenced by dry or wet climate

Table 5

Annual mean CUHI and SUHI over Beijing, Shanghai and Guangzhou from 2003 to 2016 under different climate background.

	Longitude/latitude	Air temperature (°C)	Relative humidity	Precipitation (mm)	CUHI (°C)	SUHI (°C)
Beijing	115°25'–117°30'/39°26'–41°03'	7.52 ± 0.50	5.53	526.11	1.45 ± 0.54	2.33 ± 0.18
Shanghai	120°52'–122°12'/30°40'–31°53'	13.96 ± 0.43	7.38	1114.96	0.93 ± 0.41	2.23 ± 0.11
Guangzhou	112°57'–114°3'–22°26'–23°56'	19.19 ± 0.35	7.45	1860.15	0.89 ± 0.58	2.13 ± 0.21

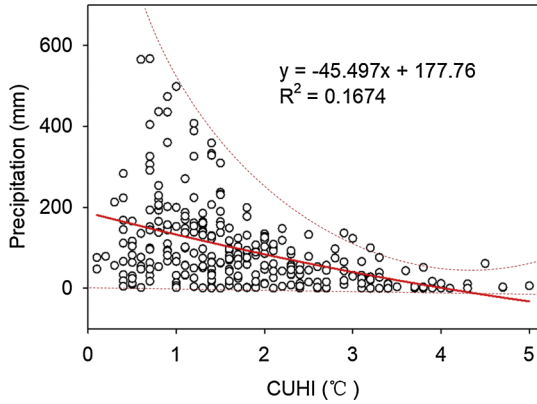


Fig. 5. The relationship between CUHI variation and monthly precipitation for all three mega-cities from 2003 to 2016. The regression line shown with red solid line was generated by using linear regression analysis between monthly CUHI and monthly precipitation. Monthly CUHI is the average value of the daily CUHI, and monthly precipitation is the sum of the daily precipitation totals for a given month. (For interpretation of the references to color in this figure legend, the reader is referred to the web version of this article.)

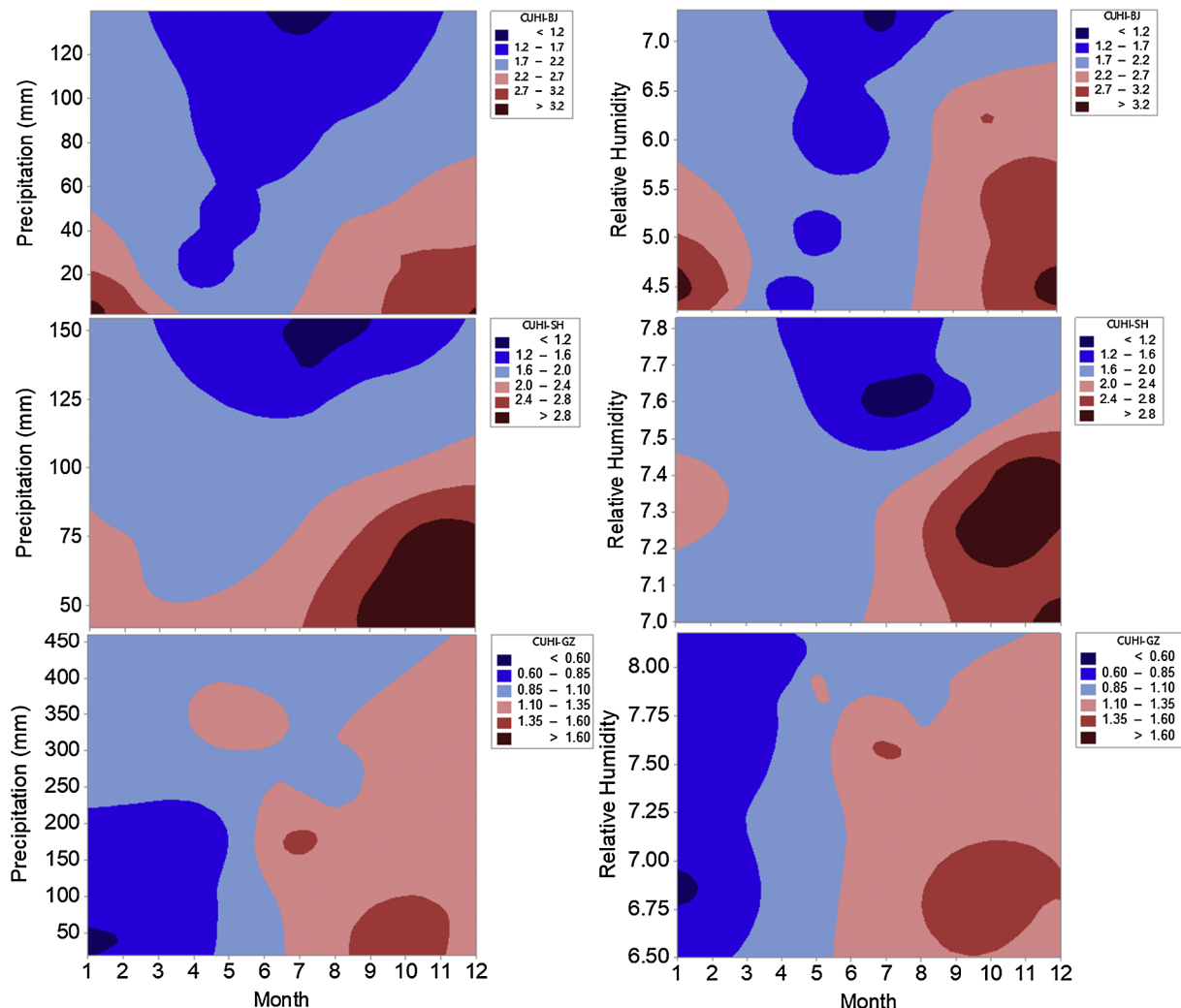


Fig. 6. Contour map of the relationship between monthly CUHI and precipitation/relative humidity in Beijing, Shanghai and Guangzhou from 2003 to 2016. The blue color means low CUHI and red color represents high CUHI, respectively. (For interpretation of the references to color in this figure legend, the reader is referred to the web version of this article.)

backgrounds. A negative relationship was detected for UHIs and precipitation across latitudes in the three mega-cities. A similar relationship was also found for UHIs and relative humidity (Table 5). For example, high CUHI ($1.45 \pm 0.54^\circ\text{C}$) and low annual precipitation (526.11 mm) was found in Beijing, whereas low CUHI ($0.89 \pm 0.58^\circ\text{C}$) and high annual precipitation (1860.15 mm) was found in Guangzhou. Wet climate could cause low SUHI and CUHI, even in cities (e.g. Guangzhou) with a warmer surface.

Negative correlation between CUHI and precipitation across three mega-cities indicated that less precipitation could result in a higher CUHI (Fig. 5). Along with the increase of CUHI, there was a clear convergent trend with precipitation decrease, suggesting that UHI or extreme heat events can mostly appear on dry days. The seasonal cycle of CUHI variation influenced by relative humidity and precipitation was analyzed (Fig. 6). As predicted, there was a large difference in CUHI across wet and dry seasons. For example, the highest CUHI in Beijing occurred in winter with the lowest relative humidity and precipitation, compared with the lowest CUHI in summer with the highest precipitation and relative humidity. This trend was also found in Shanghai with high CUHI in the dry, autumn seasons, while winter CUHI in Guangzhou was low and differed with Shanghai due to high humidity in winter. These may be partly attributed to the fact that seasonal changes of physical properties of rural surface affect surface cooling/warming,

and wet or saturated surface soil can cause an increase of absorbed solar radiation. Subsequently, UHI intensity decreased with a lower daily surface temperature range induced by a reduction of rural cooling. Larger UHI intensity in drier climate was also detected in other cities (Roth, 2007).

3.4. Implication of UHI variation across latitudes

Climatic backgrounds need to be considered when comparing UHI across latitudes. UHIs in three megacities across different latitudes and similar longitudes were investigated (Table 2). The cities are located within various climates, with a clear difference in temperature and precipitation. Results suggest that UHI changes across latitudes could be more controlled by wet or dry climates. A drier climate usually results in a higher UHI. This can be explained by the difference in the thermal capacity or thermal admittance of rural soils (Roth, 2007; Peng et al., 2012). Energy transported from urban surfaces to the urban canopy can also cause UHI variation, with faster transportation velocity resulting in higher air temperatures. Therefore, UHIs are usually higher in drier seasons. CUHI change across latitudes in the mega-cities of eastern China is negatively related to the humidity condition.

Surface properties of rural stations greatly influence UHI change. Cropland was usually the dominant land type within the rural areas, and urban expansion in the three cities was predominantly caused by the conversion of cropland to urban impervious surface. The largest proportion of cropland was found in Shanghai (56%), while Guangzhou and Beijing have larger areas of woodland (46% and 45%), with most forests around the mountains. Other land use types such as grassland or waterbodies have lower proportions in the three megacities. For example, grassland makes up less than 1% in Guangzhou and Shanghai, and waterbody makes up less than 8% in all of three cities. The decrease in UHI intensity was usually caused by increasing evapotranspiration from natural land. Meanwhile, local environmental parameters induced by land formation of inner city also changed the radiation budget in urban surface, such as urbanization significantly modifying urban morphology and surface albedo (Hu et al., 2016). Therefore, urbanization can cause an increase in average temperature in urban fringe and rural area. Air temperature of the stations surrounding urban has already been influenced by the warming effect of rapid urbanization in mega-cities (Yan et al., 2010). Satellite-based surface temperature variation was also attributed to land properties or land formation, such as green vegetation fraction and impervious surface fraction (Hu et al., 2016; Yuan and Bauer, 2007). SUHI intensity variation also depended on surface temperature from referenced land surface with different land cover types (Jin, 2012). Low SUHI intensity in winter could be due to relatively large heat capacity of rural surfaces, which absorbed high levels of incoming energy.

4. Conclusions

This study examined the relationship between UHI change and climate background by comparing SUHI and CUHI derived from satellite-based and in situ temperature data in three mega-cities of eastern China from 2003 to 2016. Strict selection procedure for urban and rural stations was conducted and the consistent temperature records for UHIs derivation were generated. We found that UHI intensity change was highly affected by heat conditions related to incoming solar radiation, with the larger land surface temperature occurring in Guangzhou (lower latitude). Meanwhile, UHI effect, including both SUHI and CUHI, in Beijing was stronger, and UHI gradually decreased in Shanghai and Guangzhou. UHI effect was also influenced by wet or dry climates with lower UHI intensity in wetter surface. Seasonal CUHI variation further indicated that UHI intensity was negatively related to monthly precipitation and relative humidity with lower CUHI in rainy season. SUHI was higher than CUHI in Guangzhou, and this effect gradually weakened in Shanghai and Beijing, especially in winter. Thus,

UHI change could be controlled by synthetic effects of heat and wet conditions in mega-cities of eastern China, and the process of heat transportation from urban surface to urban canopy may be an important factor for understanding UHI change.

We also noted that complicated UHI change were influenced by many local environment factors, especially in mega-cities experiencing the warming effect caused by urbanization in China. Our study provided a view about UHI intensity change under different climate background according to measurements from satellite and weather stations. In future, more investigations within other cities will be needed to improve our understanding of the differences between SUHI and CUHI evolution. Further, UHI intensity change from urban surface to urban canopy also requires extensive investigation by climate model simulation to understand the mechanism of heat transportation in modifying UHI effects under different climate background.

Acknowledgement

This study is supported by the CAS Strategic Priority Research Program (XDA19030401, XDA19010402, XDA2010030401), Key Laboratory of Meteorology and Ecological Environment of Hebei Province (Z201601Z), the National Natural Science Foundation of China (41861124005, 41405064). We thank Chinese Meteorological Administration and MODIS land team of NASA(<http://modis-land.gsfc.nasa.gov/>) for their released field measurements and satellite data used in our study.

References

- Arnfield, A.J., 2003. Two decades of urban climate research: A review of turbulence, exchanges of energy and water, and the urban heat island. *Int. J. Climatol.* 23, 1–26.
- Baik, J.J., Kim, Y.H., Kim, J.J., Han, J.Y., 2007. Effects of boundary-layer stability on urban heat island-induced circulation. *Theor. Appl. Climatol.* 89, 73–81.
- Bornstein, R., Styrwicki-Imamura, R., González, J.E., Lebassi, B., 2012. Interactions of Global-Warming and Urban Heat Islands in Different Climate-Zones. In: National Security and Human Health Implications of Climate Change. Springer, Netherlands, pp. 49–60.
- Buyantuyev, A., Wu, J., 2010. Urban heat islands and landscape heterogeneity: linking spatiotemporal variations in surface temperatures to land-cover and socioeconomic patterns. *Landscape Ecol.* 25, 17–33.
- Camillon, I., Barros, V., 1997. On the urban heat island effect dependence on temperature trends. *Climatic Change.* 37, 665–681.
- Chen, L., Zhu, W., Zhou, X., Zhou, Z., 2003. Characteristics of the heat island effect in Shanghai and its possible mechanism. *Adv. Atmos. Sci.* 20, 991–1001.
- Chen, X.L., Zhao, H.M., Li, P.X., Yin, Z.Y., 2006. Remote sensing image-based analysis of the relationship between urban heat island and land use/cover changes. *Remote Sens. Environ.* 104, 133–146.
- Elmes, A., Rogan, J., Williams, C., Ratnick, S., Nowak, D., Martin, D., 2017. Effects of urban tree canopy loss on land surface temperature magnitude and timing. *ISPRS J. Photogramm. Remote Sens.* 128, 338–353.
- Feng, Y., Lau, S.S.Y., Feng, Q., 2010. Summertime heat island intensities in three high-rise housing quarters in inner-city Shanghai China: Building layout, density and greenery. *Build Environ.* 45, 115–134.
- Fu, P., Weng, Q., 2018. Variability in annual temperature cycle in the urban areas of the United States as revealed by MODIS imagery. *ISPRS J. Photogramm. Remote Sens.* 146, 65–73.
- Gedzelman, S.D., Austin, S., Cermak, R., Stefano, N., Partridge, S., Quesenberry, S., Robinson, D.A., 2003. Mesoscale aspects of the urban heat island around New York City. *Theor. Appl. Climatol.* 75, 29–42.
- Holderness, T., Barr, S., Dawson, R., Hall, J., 2013. An evaluation of thermal Earth observation for characterizing urban heatwave event dynamics using the urban heat island intensity metric. *Int. J. Remote Sens.* 34, 864–884.
- Hu, L., Brunsell, N.A., 2013. The impact of temporal aggregation of land surface temperature data for surface urban heat island SUHI monitoring. *Remote Sens. Environ.* 134, 162–174.
- Hu, Y., Jia, G., Pohl, C., Zhang, X., Van Genderen, J., 2016. Assessing surface albedo change and its induced radiation budget under rapid urbanization with Landsat and GLASS data. *Theor. Appl. Climatol.* 123, 711–722.
- Hu, Y.H., Jia, G.S., 2010. Influence of land use change on urban heat island derived from multi-sensor data. *Int. J. Climatol.* 30, 1382–1395.
- Huang, X., Wang, Y., 2019. Investigating the effects of 3D urban morphology on the surface urban heat island effect in urban functional zones by using high-resolution remote sensing data: a case study of wuhan, Central China. *ISPRS J. Photogramm. Remote Sens.* 152, 119–131.
- Jin, M.L., Dickinson, R.E., 2010. Land surface skin temperature climatology: benefitting from the strengths of satellite observations. *Environ. Res. Lett.* 5, 044004.
- Jin, M.S., 2012. Developing an index to measure urban heat island effect using satellite

- land skin temperature and land cover observations. *J. Climate*. 25, 6193–6201.
- Jin, M.S., Kessomkiat, W., Pereira, G., 2011. Satellite-observed urbanization characters in shanghai, china: aerosols, urban heat island effect, and land-atmosphere interactions. *Remote Sens.* 3, 83–99.
- Lai, J., Zhan, W., Huang, F., Quan, J., Hu, L., Gao, L., Ju, W., 2018. Does quality control matter? Surface urban heat island intensity variations estimated by satellite-derived land surface temperature products. *ISPRS J. Photogramm. Remote Sens.* 139, 212–227.
- Lazzarin, M., Marpu, P.R., Ghedira, H., 2013. Temperature-land cover interactions: the inversion of urban heat island phenomenon in desert city areas. *Remote Sens. Environ.* 130, 136–152.
- Li, J., Song, C., Cao, L., Zhu, F., Meng, X., Wu, J., 2011. Impacts of landscape structure on surface urban heat islands: a case study of Shanghai, China. *Remote Sens. Environ.* 115, 3249–3263.
- Liu, J.Y., Tian, H.Q., Liu, M.L., Zhuang, D.F., Melillo, J.M., Zhang, Z.X., 2005. China's changing landscape during the 1990s: large-scale land transformations estimated with satellite data. *Geophys. Res. Lett.* 32, L02405.
- Liu, W., Ji, C., Zhong, J., Jiang, X., Zheng, Z., 2007. Temporal characteristics of the Beijing urban heat island. *Theor. Appl. Climatol.* 87, 213–221.
- Maimaitiyiming, M., Ghulam, A., Tiyip, T., Pla, F., Latorre Carmona, P., Halik, Ü., Sawut, M., Caetano, M., 2014. Effects of green space spatial pattern on land surface temperature: Implications for sustainable urban planning and climate change adaptation. *ISPRS J. Photogramm. Remote Sens.* 89, 59–66.
- Miao, S., Chen, F., Lemone, M.A., Tewari, M., Li, Q., Wang, Y., 2009. An Observational and modeling study of characteristics of urban heat island and boundary layer structures in Beijing. *J. Appl. Meteorol. Clim.* 48, 484–501.
- Mohsin, T., Gough, W.A., 2012. Characterization and estimation of urban heat island at Toronto: impact of the choice of rural sites. *Theor. Appl. Climatol.* 108, 105–117.
- Oke, T.R., Taesler, R., Olsson, I.E., 1991. The tropical urban climate experiment truce. *Energ. Buildings*. 15, 67–73.
- Peng, S., Piao, S., Ciais, P., Friedlingstein, P., Ottle, C., Breon, F., Nan, H., Zhou, L., Myneni, R.B., 2012. Surface urban heat island across 419 global big cities. *Environ. Sci. Technol.* 46, 696–703.
- Roth, M., 2007. Review of urban climate research in subtropical regions. *Int. J. Climatol.* 27, 1859–1873.
- Sarrat, C., Lemonsu, A., Masson, V., Guedalia, D., 2006. Impact of urban heat island on regional atmospheric pollution. *Atmos. Environ.* 40, 1743–1758.
- Stewart, I.D., 2011. A systematic review and scientific critique of methodology in modern urban heat island literature. *Int. J. Climatol.* 31, 200–217.
- Stewart, I.D., Oke, T.R., 2012. Local climate zones for urban temperature studies. *B. Am. Meteorol. Soc.* 93, 1879–1900.
- Streutker, D.R., 2003. Satellite-measured growth of the urban heat island of Houston, Texas. *Remote Sens. Environ.* 85, 282–289.
- Tran, D.X., Pla, F., Latorre Carmona, P., Myint, S.W., Caetano, M., Kieu, H.V., 2017. Characterizing the relationship between land use/land cover change and land surface temperature. *ISPRS J. Photogramm. Remote Sens.* 124, 119–132.
- United Nations, 2018. World urbanization prospects: The 2018 revision. New York.
- Voogt, J.A., Oke, T.R., 1998. Effects of urban surface geometry on remotely-sensed surface temperature. *Int. J. Remote Sens.* 19, 895–920.
- Voogt, J.A., Oke, T.R., 2003. Thermal remote sensing of urban climates. *Remote Sens. Environ.* 86, 370–384.
- Wan, Z.M., 2008. New refinements and validation of the MODIS land-surface temperature/emissivity products. *Remote Sens. Environ.* 112, 59–74.
- Wang, J., Huang, B., Fu, D., Atkinson, P.M., 2015. Spatiotemporal variation in surface urban heat island intensity and associated determinants across major Chinese Cities. *Remote Sens.* 7, 3670–3689.
- Wang, K., Jiang, S., Wang, J., Zhou, C., Wang, X., Lee, X., 2017. Comparing the diurnal and seasonal variabilities of atmospheric and surface urban heat islands based on the Beijing urban meteorological network. *J. Geophys. Res.-Atmos.* 122, 2131–2154.
- Weng, Q., 2012. Remote sensing of impervious surfaces in the urban areas: requirements, methods, and trends. *Remote Sens. Environ.* 117, 34–49.
- Weng, Q., Lu, D., Schubring, J., 2015. Estimation of land surface temperature–vegetation abundance relationship for urban heat island studies. *Remote Sens. Environ.* 89, 467–483.
- Weng, Q.H., 2003. Fractal analysis of satellite-detected urban heat island effect. *Photogramm. Eng. Rem. S.* 69, 555–566.
- Weng, Q.H., Lu, D.S., Schubring, J., 2004. Estimation of land surface temperature–vegetation abundance relationship for urban heat island studies. *Remote Sens. Environ.* 89, 467–483.
- Wu, J., Chow, K., Fung, J.C.H., Lau, A.K.H., Yao, T., 2011. Urban heat island effects of the Pearl River Delta city clusters—their interactions and seasonal variation. *Theor. Appl. Climatol.* 103, 489–499.
- Wu, K., Yang, X., 2013. Urbanization and heterogeneous surface warming in eastern China. *Chinese Sci. Bull.* 58, 1363–1373.
- Yan, Z., Li, Z., Li, Q., Jones, P., 2010. Effects of site change and urbanisation in the Beijing temperature series 1977–2006. *Int. J. Climatol.* 30, 1226–1234.
- Yu, S.Q., Bian, L., Lin, X.C., 2005. Changes in the spatial scale of Beijing UHI and urban development. *Sci. China Earth Sci.* 482, 116–127.
- Yuan, F., Bauer, M.E., 2007. Comparison of impervious surface area and normalized difference vegetation index as indicators of surface urban heat island effects in Landsat imagery. *Remote Sens. Environ.* 106, 375–386.
- Zhang, Z., Wang, X., Zhao, X., Liu, B., Yi, L., Zuo, L., Wen, Q., Liu, F., Xu, J., Hu, S., 2014. A 2010 update of National Land Use/Cover Database of China at 1:100000 scale using medium spatial resolution satellite images. *Remote Sens. Environ.* 149, 142–154.
- Zhao, L., Lee, X., Smith, R.B., Oleson, K., 2014. Strong contributions of local background climate to urban heat islands. *Nature*. 511, 216.